

A *K*-Band-Frequency Agile Microstrip Bandpass Filter Using a Thin-Film HTS/Ferroelectric/Dielectric Multilayer Configuration

Guru Subramanyam, *Senior Member, IEEE*, Frederick W. Van Keuls, *Member, IEEE*, and Félix A. Miranda, *Senior Member, IEEE*

Abstract—In this paper, we report on $\text{YBa}_2\text{Cu}_3\text{O}_{7-\delta}$ (YBCO) thin-film/ SrTiO_3 (STO) thin-film *K*-band tunable bandpass filters on LaAlO_3 (LAO) dielectric substrates. The two-pole filter has a center frequency of 19 GHz and a 4% bandwidth. Tunability is achieved through the nonlinear dc electric-field dependence of the relative dielectric constant of STO ($\epsilon_{r,\text{STO}}$). A large tunability ($\Delta f/f_o = (f_{V,\text{max}} - f_o)/f_o$, where f_o is the center frequency of the filter at no bias and $f_{V,\text{max}}$ is the center frequency of the filter at the maximum applied bias) of greater than 10% was obtained in YBCO/STO/LAO microstrip bandpass filters operating below 77 K. A center frequency shift of 2.3 GHz (i.e., a tunability factor of approximately 15%) was obtained at a 400-V bipolar dc bias, and 30 K, with minimal degradation in the insertion loss of the filter. This paper addresses design, fabrication, and testing of tunable filters based on STO ferroelectric thin films. The performance of the YBCO/STO/LAO filters is compared to that of gold/STO/LAO counterparts.

Index Terms—*K*-band frequencies, microstrip filters, STO ferroelectric thin films, tunable filters, YBCO HTS thin films.

I. INTRODUCTION

PLANAR microstrip high-temperature superconductor (HTS) filters are currently being tested by the wireless communications industry [e.g., cellular and personal communication system (PCS)] for low-loss high-performance receiver front ends [1], [2]. Initial applications of the HTS thin-film microstrip filters have been successful, exhibiting superior performance (e.g., lower insertion loss and steeper out-of-band rejection) than their gold-based counterparts. In the satellite communications arena, more applications are evolving at frequencies above the traditionally used *C*-band (\sim 4–7 GHz), in which the integration of HTS is attractive due to the high-quality epitaxial HTS thin films currently available

[3], [4]. However, one of the factors that have slowed down the integration of HTS thin films into microwave communication circuits is that, notwithstanding careful design and fabrication, only rarely can one meet the desired performance specifications consistently. For filter applications, this limitation is compensated by tuning the filter either through mechanical means (i.e., with tuning screws) or other coupling mechanisms. On the other hand, if electronic tuning is incorporated into these filter circuits, allowing their tuning over a broad-band range to meet the desired specifications, this will greatly improve the practical applicability of HTS circuits.

Frequency and phase agility in microwave circuits can be realized using ferroelectric- or ferrite-based thin films incorporated into conventional microstrip circuits [5]–[8]. Novel superconductor-ferrite phase shifters and circulators have been demonstrated recently, with magnetic flux confinement [6]. However, usage of ferrite thin films requires external coils and typically large currents for tunability. Ferroelectric thin films are very attractive due to their electrical tunability of the relative dielectric constant. Ferroelectric thin films are frequency agile due to the nonlinear dc electric-field dependence of their relative dielectric constant. Strontium titanate (SrTiO_3) and barium strontium titanate ($\text{Ba}_x\text{Sr}_{1-x}\text{TiO}_3$) are two of the most popular ferroelectric thin films currently being studied. It has been demonstrated that the SrTiO_3 's (hereupon STO) relative dielectric constant ($\epsilon_{r,\text{STO}}$) could be reduced by more than a factor of five under the influence of a dc electric field below 77 K [9]. A $\text{YBa}_2\text{Cu}_3\text{O}_{7-\delta}$ (YBCO)/STO/lanthanum aluminate (LaAlO_3 , hereafter referred to as LAO) coplanar bandpass filter designed for 2.5 GHz has been demonstrated by Findikoglu *et al.* [10]. A large tunability factor above 15% was demonstrated in these filters and the results indicated that tuning resulted in improved filter characteristics.

Recently, we have demonstrated tunability in a conductor/STO/LAO multilayered microstrip bandpass filter at *K*-band frequencies [11], [12]. In this paper, we report on the two-pole tunable YBCO/STO multilayered microstrip bandpass filters on LAO substrates. The experimental performance of these filters is compared to that of their gold/STO/LAO counterparts, and demonstrates the feasibility of this technology for applications in *K*-band satellite communication subsystems such as a receiver front-end.

Manuscript received November 19, 1998. The work of G. Subramanyam was supported by NASA/OAI under 1997 and 1998 Summer Faculty Fellowships at NASA Glenn Research Center, and by the University of Northern Iowa under a 1997–1998 Applied Technology Research Grant. The work of F. W. Van Keuls was supported by the National Research Council under a fellowship. An earlier version of this work was presented at the 1998 IEEE Microwave Theory and Techniques Society (MTT-S) International Microwave Symposium.

G. Subramanyam is with the Department of Electrical and Computer Engineering, University of Dayton, Dayton, OH 45469 USA.

F. W. Van Keuls and F. A. Miranda are with the NASA Glenn Research Center, Cleveland, OH 44135 USA.

Publisher Item Identifier S 0018-9480(00)02773-3.

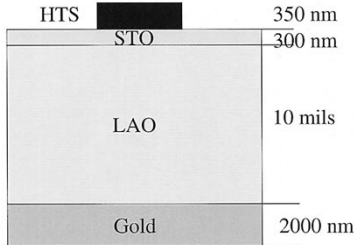


Fig. 1. Geometry of the multilayered microstrip structure. The thickness of the top conductor was $0.35 \mu\text{m}$ for HTS thin film and $2.0 \mu\text{m}$ for gold.

II. DESIGN OF THE TUNABLE MICROSTRIP FILTER

The two-pole bandpass filter was designed using microstrip edge-coupled resonators. The filter was designed for a center frequency of 19 GHz, with 4% bandwidth, and a passband ripple below 0.5 dB. The cross section of the multilayered microstrip structure is shown in Fig. 1. The multilayered microstrip structure consists of an LAO substrate ($254\text{-}\mu\text{m}$ thick), a 300-nm-thick STO layer, a $0.35\text{-}\mu\text{m}$ -thick YBCO thin film for the HTS microstrip, and $2\text{-}\mu\text{m}$ -thick gold ground plane. The gold/STO/LAO filter had a $2\text{-}\mu\text{m}$ gold thin film for the conductor with the other layers being the same as for the HTS filter. The geometry of the multilayered microstrip was simulated using Sonnet's electromagnetic (em) simulator to obtain the relationships between the effective dielectric constant (ϵ_{eff}) of the structure and the characteristic impedance (Z_0) for the tunable range of $\epsilon_{r\text{STO}}$. The tunable range of $\epsilon_{r\text{STO}}$ was chosen to be between 3000 at zero field to 300 at high field and 77 K, based on the data obtained from low-frequency capacitance measurements on test structures [9], [13]. The extracted results provided the basis for the calculation of tunability factor that can be obtained using this multilayered microstrip structure. The frequency-dependent ϵ_{eff} and Z_0 of the microstrip are plotted versus the tunable range of the $\epsilon_{r\text{STO}}$ at a fixed frequency of 20 GHz in Fig. 2(a) and (b). Large variations of ϵ_{eff} and Z_0 at 20 GHz are evident with the electrically tunable range of $\epsilon_{r\text{STO}}$ for $w/h = 0.1$ and 0.3 . The tunable range of $\epsilon_{r\text{STO}}$ is only valid for the temperature dependence of $\epsilon_{r\text{STO}}$. The bias-dependent $\epsilon_{r\text{STO}}$ is not easy to model using Sonnet's em because of the spatial variation of the dc bias, $\epsilon_{r\text{STO}}$ varies as one moves farther away from the microstrip line. The assumed values for tunable range of $\epsilon_{r\text{STO}}$ nevertheless provide a meaningful calculation for the tunability factor in this multilayered microstrip structure.

The filters were designed using identical quarter-wavelength coupled microstrip resonator sections designed for $50\text{-}\Omega$ characteristic impedance. The coupling is achieved through the fringing fields of adjacent resonator sections. The coupled sections were designed using the 0.2-dB ripple Chebyshev filter design procedure [14], [15]. To reduce the bandwidth, the spacing between the input and output sections was increased by the use of 45° angular coupled sections. For the dc biasing of the filters, radial stubs were designed for each of the resonator sections. The radial stubs were designed for low insertion loss over the bandwidth of interest [16]. The bias stubs provide means for individually controlling the poles using the electric field between the coupled lines. The design was optimized

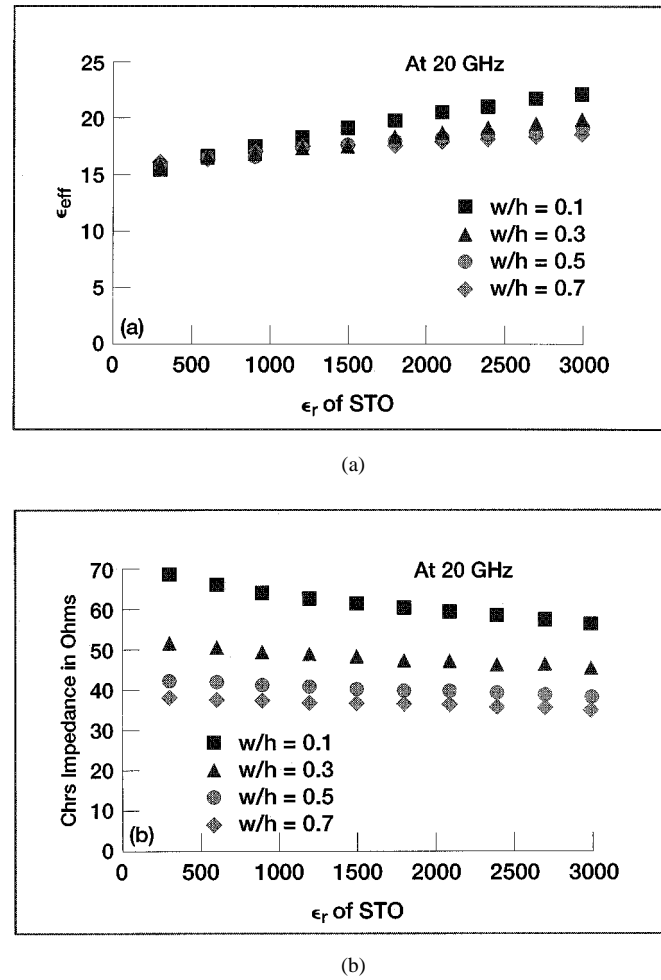


Fig. 2. Theoretical simulation results for: (a) the effective dielectric constant and (b) the characteristic impedance of the multilayered microstrip structure versus the relative dielectric constant of STO for different W/H . The thickness of STO was assumed as 300 nm. The loss tangent of STO was assumed to be 0.01. The tunable range of $\epsilon_{r\text{STO}}$ was assumed to be between 300–3000.

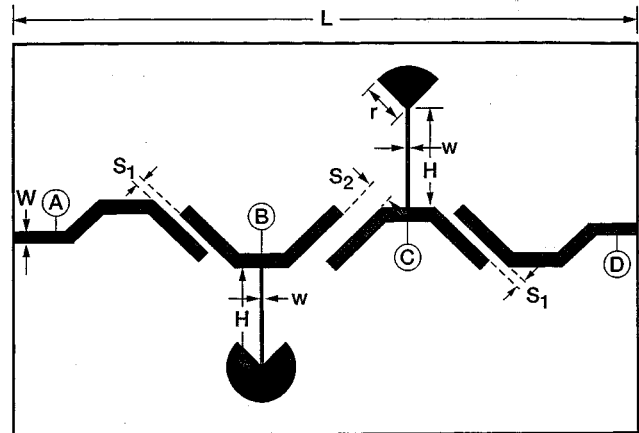


Fig. 3. Optimized geometry of the ferroelectric tunable bandpass filter. The dimensions are: $W = 80 \mu\text{m}$, $L = 6.8 \text{ mm}$, $S_1 = 100 \mu\text{m}$, $S_2 = 300 \mu\text{m}$, $w = 12.5 \mu\text{m}$, $H = 1.33 \text{ mm}$, and $r = 200 \mu\text{m}$.

using Sonnet's em analysis computer-aided engineering (CAE) package [17]. The geometry of the optimized filter circuit is shown in Fig. 3. Sonnet's em simulation results for the

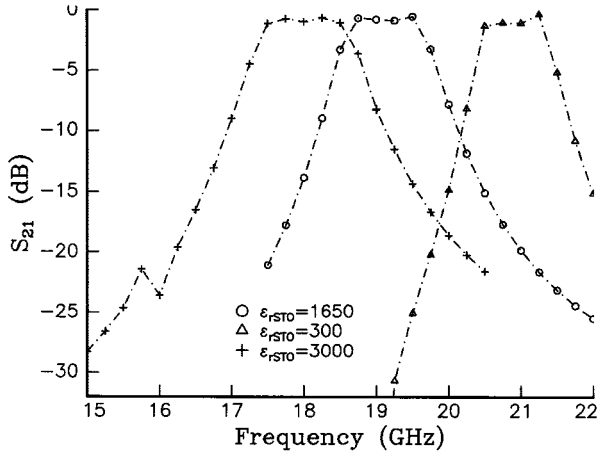


Fig. 4. Theoretical simulation results for the HTS/STO/LAO filters with bias stubs. Note that the insertion loss does not vary appreciably in the entire tuning range of $\epsilon_{r,\text{STO}}$.

YBCO multilayered microstrip bandpass filter are shown in Fig. 4, for the cases of $\epsilon_{r,\text{STO}}$ equal to 300, 1650, and 3000. The loss tangent ($\tan \delta$) of the STO films was assumed to be 0.01. Since the $\epsilon_{r,\text{STO}}$ could be varied between 300–3000 at 77 K [9], the filter was designed for normal operation at $\epsilon_{r,\text{STO}} = 1650$ (approximate midpoint value of $\epsilon_{r,\text{STO}}$) so that its passband can be electronically tuned to lower or higher frequencies. However, one must note that while Sonnet's em analysis assumes that $\epsilon_{r,\text{STO}}$ is the same across the sample, in reality, biasing the microstrip causes local changes in $\epsilon_{r,\text{STO}}$. As mentioned before, this limitation may introduce discrepancies between the modeled and experimental data under bias. The modeled data for the HTS filter's insertion loss at 77 K was below 0.7 dB in the worst case, and did not change appreciably, as the $\epsilon_{r,\text{STO}}$ was changed from 300 to 3000. The bandwidth of the filter was worse for $\epsilon_{r,\text{STO}} = 3000$, compared to $\epsilon_{r,\text{STO}} = 300$. As shown in Fig. 4, the filter could be tuned between 17.5–20.5 GHz. The simulation of the gold circuit yielded similar tunability, but the insertion loss was approximately 2 dB in the passband, and did not change appreciably with the $\epsilon_{r,\text{STO}}$. The theoretical results indicated that the return loss in the passband was better than 20 dB for both HTS and gold circuits.

III. EXPERIMENTAL

The YBCO/STO/LAO samples used in this study were obtained from Superconductor Core Technologies (SCT), Golden, CO. Both the superconducting and ferroelectric films were deposited by laser ablation. The deposition and post annealing techniques for the STO and YBCO thin films have been thoroughly discussed elsewhere [9]. The YBCO microstrip bandpass filter circuit was fabricated at SCT using a dry chemical etching technique [9]. A liftoff photolithography technique was used at the NASA Glenn Research Center, Cleveland, OH, for the fabrication of the gold microstrip filter circuit. A 2- μm gold ground plane was deposited to complete the circuit fabrication. The circuits were packaged for testing of the filter's swept frequency S -parameters in a helium-gas closed-cycle cryogenic system. For studying the tunability of the circuits, the resonator

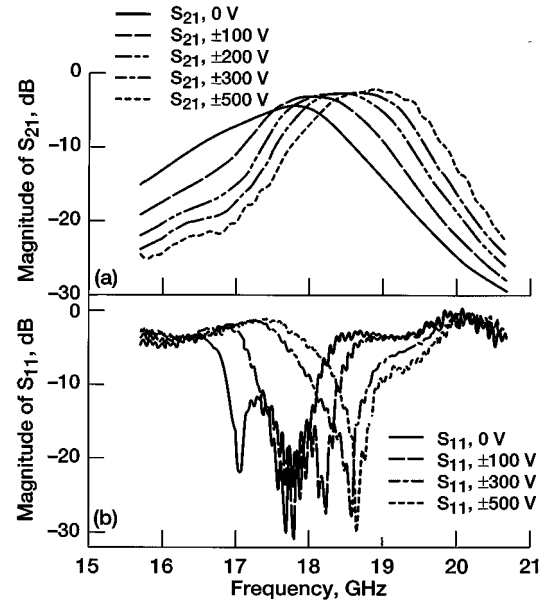


Fig. 5. Bias dependence of S_{21} and S_{11} for an HTS/STO/LAO filter at 77 K, under full bipolar bias configuration.

sections needed to be electrically biased. To apply the bias, gold wire bonds were attached to the bias pads using an ultrasonic wire bonder. Tunability of the filter circuits were studied using both unipolar and bipolar biasing schemes. For unipolar biasing scheme, nodes A and C were connected to positive bias, with nodes B and D tied to zero bias or ground (see Fig. 3). For bipolar biasing, nodes A and C were connected to the positive bias, and nodes B and D were connected to a negative bias of the same magnitude. The magnitude of the dc bias was increased from 0 to 400 V in steps of 50 V for the bipolar biasing scheme. The bipolar bias tunes each pole uniformly with respect to ground while maintaining a large electric field across the gaps. This biasing scheme gave superior tuning and more symmetric passbands. Since circuit geometries result in unequal electric fields in different portions of the circuit, the maximum applied electric field becomes an important parameter. We denote this as the peak electric field E_{PEAK} . In our filter circuit, the largest electric field due to the applied bias is experienced across the input and output coupling gaps. Although the bias voltage is large, the peak electric field strengths do not exceed 10^5 V/cm, remaining below the breakdown strength of STO ($\sim 4 \times 10^5$ V/cm) [18].

IV. RESULTS AND DISCUSSIONS

The first set of HTS tunable filter circuits exhibited higher insertion losses compared to the theoretical simulation results. The lowest passband insertion loss measured was approximately 1.5 dB at 24 K, which is higher than the simulation results. These represent nondeembedded data (i.e., it includes the losses due to the coaxial-to-microstrip transitions) and, therefore, the intrinsic insertion loss of the filter is expected to be lower. The bias dependence of S_{21} and S_{11} for one of the filters with bias stubs, denoted as sample 1, is shown in Fig. 5. The unbiased filter's passband at 77 K was centered at 17.4 GHz, with return losses better than 10 dB in the passband. The bandwidth of the

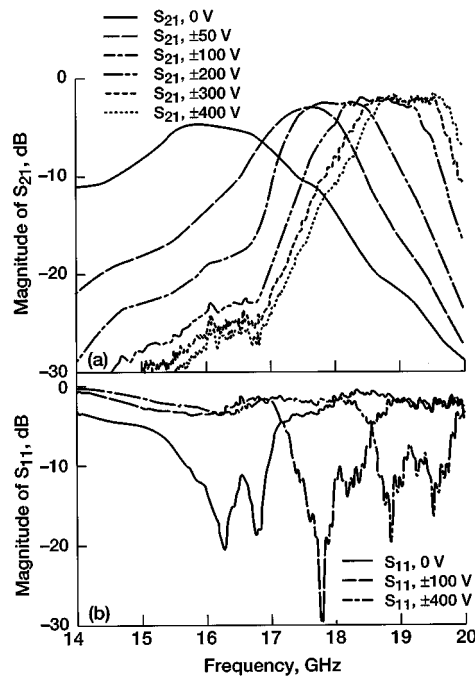


Fig. 6. The bias dependence of S_{21} and S_{11} for the same filter in Fig. 5, at 24 K under full bipolar configuration.

circuit was 7%, higher than the design bandwidth of 4% at 77 K. The passband ripple was also larger, with rounded edges instead of sharper skirts. The point of minimum insertion loss was approximately 3.3 dB, at 77 K, for the unbiased filter. The field dependence of the filter's S_{21} and S_{11} at 77 K were measured at an input power level of +10 dBm. The center frequency of the circuit shifted from 17.4 GHz at no bias, to 19.1 GHz at ± 500 -V bias, a tunability of 9% at 77 K. Note that the passband insertion loss and the bandwidth improve with increasing bipolar bias voltage. The same filter was tested at 24 K, near the maximum ϵ_r of the STO thin film. Fig. 6 shows the bias dependence of the filter at 24 K. The filter at zero bias had a center frequency close to 16.25 GHz and poor out-of-band rejection characteristics. At zero bias, the minimum passband insertion loss was 4.4 dB. The return losses seem to be sensitive to the temperature of operation, showing slight improvement at 77 K (Fig. 5), while degrading at 24 K (Fig. 6) under the influence of the applied bias. The greater frequency shift and losses at lower temperatures are due to this temperature being closer to the maximum of ϵ_r and $\tan \delta$, respectively. Unlike bulk STO, thin STO films exhibit a maximum ϵ_r and $\tan \delta$ within the 20–50-K temperature range. Similar to the case at 77 K, increasing the bipolar bias up to ± 400 V resulted in a center frequency shift of 2.6 GHz. The tunability factor is greater than 14% at 24 K. The passband insertion loss at 24 K improved to 1.5 dB at a bipolar bias of ± 200 V. The passband insertion loss, reflection loss, bandwidth, and filter's out-of-band rejection characteristics improved at 24 K with increasing bipolar bias. For this filter, the largest change in center frequency and insertion loss per applied dc voltage occurs within the first ± 50 V. Another HTS filter, denoted as sample 2, was tested at 30 K and exhibited a bipolar bias tunability as shown in Fig. 7. The filter's passband shifted from a center frequency of 16.5 GHz at

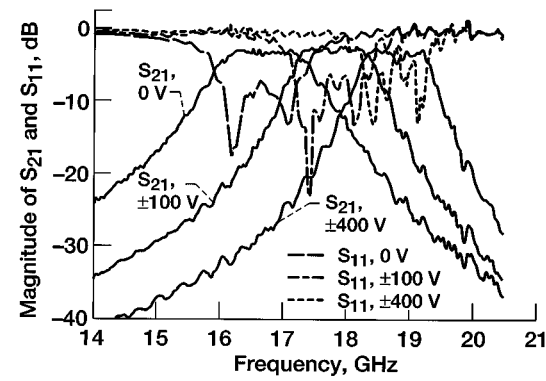


Fig. 7. Bias dependence of S_{21} and S_{11} for another HTS/STO/LAO filter at 30 K under full bipolar configuration.

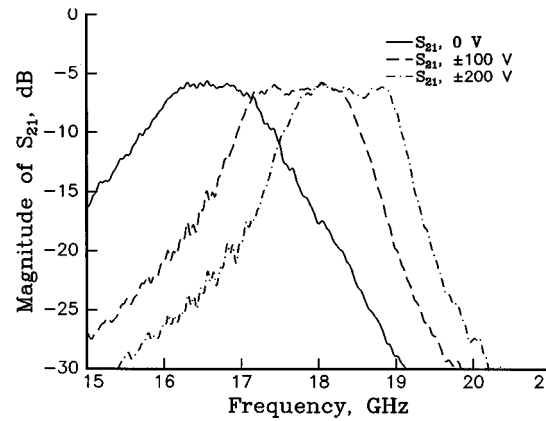


Fig. 8. Bias dependence of a gold/STO/LAO filter at 77 K. Note that the insertion loss of gold/STO/LAO filter is higher than the HTS counterparts.

no bias to 18.8 GHz at the maximum applied bias of ± 400 V, a tunability factor greater than 12%. The filter's passband insertion loss remained relatively the same through the tuning range. Remarkably, all of the filters tested to date have shown large tunability factors ($\geq 9\%$) at and below 77 K.

For comparison, gold/STO/LAO microstrip filter circuits were tested for electrical tunability at temperatures below 77 K. The center frequency of the circuit shifted from 18.1 to 19.0 GHz, a tunability factor of approximately 4%, at 77 K, under unipolar biasing [11]. The tunability improved to 8% at 40 K. Fig. 8 shows the electrical tunability of a gold/STO/LAO biased using the bipolar biasing scheme. A tunability of approximately 11% was obtained at 40 K and at a dc bias of ± 200 V. This tunability is comparable to that exhibited by the YBCO/STO/LAO filters. The insertion loss exhibited by this filter was approximately 6 dB, compared to less than 2 dB for HTS counterparts.

The center frequency shift is defined as $(f_{V \text{ max}} - f_0)$, where $f_{V \text{ max}}$ is the center frequency at maximum applied bias voltage, and f_0 is the center frequency at no bias. The center frequency shift versus the peak electric field (E_{PEAK}) for the HTS/STO/LAO filters is shown in Fig. 9. The samples were tuned using the bipolar biasing scheme. As seen in the figure, sample 1 at 24 K has the largest tunability. Fig. 10 shows the electric-field dependence of insertion loss for the same set of HTS/STO/LAO filters. Normally, it will be advantageous if the

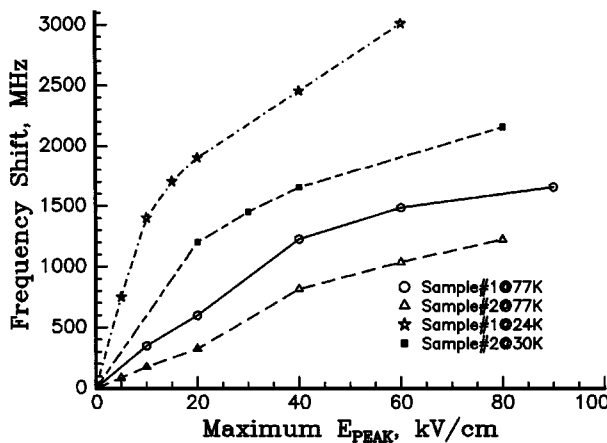


Fig. 9. Electric-field dependence of shift in center frequency for the same set of HTS/STO/LAO filters. The largest electric field for any given bipolar bias voltage is experienced across the input and output coupling gaps, and is denoted as E_{PEAK} .

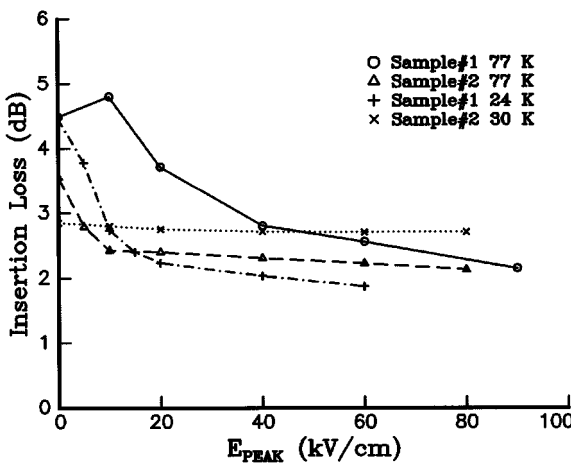


Fig. 10. Electric-field dependence of the insertion loss for the same set of HTS/STO/LAO filters. At E_{PEAK} values above 40 kV/cm, the change in insertion loss is very minimal.

insertion loss does not vary much with the applied electric field. In sample 1, which offered the largest tunability, the insertion loss varies by several decibels from zero field condition to the E_{PEAK} value of 40 kV/cm. In contrast, sample 2, which is less tunable compared to sample 1, offers low insertion-loss variation with increasing E_{PEAK} . It is evident that the insertion loss does not change appreciably above the E_{PEAK} value of 40 kV/cm. The results presented in Figs. 9 and 10 are significant, as one could compare different geometry tunable filters for variation in tunability as well as insertion loss for the range of applied electric-field strengths.

As mentioned earlier in this paper, the higher insertion losses encountered in YBCO/STO/LAO filters with respect to the modeled values are partially due to the nondeembedded nature of the experimental data. In addition, when comparing the modeled and experimental data, one should realize that Sonnet's em analysis assumes ϵ_r to be the same across the sample, while in reality, biasing the microstrip causes local

changes in ϵ_r and $\tan \delta$. Other factors such as the HTS thin-film quality or higher than expected $\tan \delta$ of STO may also contribute adversely to the measured insertion losses. The unloaded Q of the HTS resonator sections in the filters was estimated to be approximately 200 based on the model given in [14], which could possibly be improved by process optimization. The major limiting factor for the unloaded Q is the dielectric losses in the STO layer. Measurements of $\tan \delta$ values for laser-ablated STO thin films at cryogenic temperatures and gigahertz frequencies range from 0.005 to 0.05 [13], [19].

The impact of these filters can be measured at the component level as well as the subsystem level. At the component level, the filter's frequency agility allows for adjusting for Doppler effects, frequency hopping, and other communication applications requiring filter's passband reconfiguration. In addition, using a single tunable filter rather than the use of filter banks can greatly reduce size and weight without sacrificing performance. Also, low cost, ease of fabrication, and planar geometry make this filter technology very appealing for insertion into satellite receiver front-ends. Note that, even for the insertion losses measured in this study, potential insertion of these filters in receiver front-ends appears to be feasible at the expense of moderate tradeoffs in the antenna's area. Of course, insertion of the cryocooling technology introduces a hurdle. However, efforts are underway by commercial industry to reduce the size and power consumption of the cryocoolers. Also, there is a great deal of work being performed to optimize other ferroelectric materials (e.g., $\text{Ba}_x\text{Sr}_{1-x}\text{TiO}_3$) that can enable the realization of this technology at room temperature.

V. CONCLUSION

In summary, a planar tunable microstrip bandpass filter with low insertion loss has been realized using a thin-film YBCO and a nonlinear dielectric STO ferroelectric thin film. Experimental results indicated greater than 12% tunability at temperatures below 77 K using the electric field dependence of the ϵ_r . The YBCO/STO/LAO filters showed lower losses compared to gold-based circuits. The experimental verification of these filters demonstrates the feasibility of this technology for applications in *K*-band satellite communication subsystems such as a receiver front-end.

ACKNOWLEDGMENT

This work was performed at the NASA Glenn Research Center, Cleveland, OH. The authors thank SCT for the samples used in this research.

REFERENCES

- [1] R. Keenan, "Superconductors improve base-station sensitivity," in *Wireless Syst. Design*, July 1997, p. 32.
- [2] H. Moritz, "Filter brings coverage without interference," *Wireless Business Technol.*, vol. 4, pp. 82–83, 1998.
- [3] R. S. Kwok, S. J. Fiedzusko, F. A. Miranda, G. V. León, M. S. Demo, and D. Y. Bohman, "Miniaturized HTS/dielectric multilayer filters for satellite communications," *IEEE Trans. Appl. Superconduct.*, vol. 7, pp. 3706–3709, June 1997.

- [4] H. H. S. Javadi, J. G. Bowen, D. L. Rascoe, R. R. Romanofsky, C. M. Chorey, and K. B. Bhasin, "Jet Propulsion Laboratory/NASA Lewis Research Center space qualified hybrid high temperature superconducting/semiconducting 7.4 GHz low noise downconverter for NRL HTSSE-II Program," *IEEE Trans. Microwave Theory Tech.*, vol. 44, pp. 1279–1288, July 1996.
- [5] O. G. Vendik, L. T. Ter-Martirosyan, A. I. Dedyk, S. F. Karmanenko, and R. A. Chakalov, "High T_c superconductivity: New applications of ferroelectrics at microwave frequencies," *Ferroelect.*, vol. 144, pp. 33–43, 1993.
- [6] D. E. Oates, A. Piqué, K. S. Harshavardhan, J. Moses, F. Yang, and G. F. Dionne, "Tunable YBCO resonators on YIG substrates," *IEEE Trans. Appl. Superconduct.*, vol. 7, pp. 2338–2342, June 1997.
- [7] A. M. Hermann, R. M. Yandrofski, J. F. Scott, A. Naziripour, D. Galt, J. C. Price, J. Cuchario, and R. K. Ahrenkiel, "Oxide superconductors and ferroelectrics-materials for a new generation of tunable microwave devices," *J. Superconduct.*, vol. 7, no. 2, pp. 463–469, 1994.
- [8] S. S. Gevorgian, D. I. Kaparkov, and O. G. Vendik, "Electrically controlled HTSC/ferroelectric coplanar waveguide," *Proc. Inst. Elect. Eng.*, vol. 141, pp. 501–503, 1994.
- [9] F. A. Miranda, R. R. Romanofsky, F. W. Van Keuls, C. H. Mueller, R. E. Treece, and T. V. Rivkin, "Thin film multi-layer conductor/ferroelectric tunable microwave components for communication applications," *Integrated Ferroelect.*, vol. 17, pp. 231–246, 1997.
- [10] A. T. Findikoglu, Q. X. Jia, X. D. Wu, G. J. Chen, T. Venkatesan, and D. W. Reagor, "Tunable and adaptive bandpass filter using a nonlinear dielectric thin film of STO," *Appl. Phys. Lett.*, vol. 68, no. 12, pp. 1651–1653, 1996.
- [11] G. Subramanyam, F. W. Van Keuls, and F. A. Miranda, "A novel K -band tunable microstrip bandpass filter using a HTS/ferroelectric/dielectric multilayer configuration," *IEEE MTT-S Int. Microwave Symp. Dig.*, vol. 2, pp. 1011–1014, 1998.
- [12] ———, "A K -band tunable microstrip bandpass filter using a thin film conductor/ferroelectric/dielectric multilayer configuration," *IEEE Microwave Guided Wave Lett.*, vol. 8, pp. 78–80, Feb. 1998.
- [13] M. J. Dalberth, R. E. Stauben, J. C. Price, C. T. Rogers, and D. Galt, "Improved low frequency and microwave dielectric response in strontium titanate thin films grown by pulsed laser ablation," *Appl. Phys. Lett.*, vol. 72, pp. 507–509, 1998.
- [14] G. Matthaei, L. Young, and E. M. T. Jones, *Microwave Filters, Impedance-Matching Networks, and Coupling Structures*. Norwood, MA: Artech House, 1980.
- [15] T. Edwards, *Foundations of Microstrip Circuit Design*. New York: Wiley, 1992.
- [16] V. Sadhir and I. Bahl, "Radial line structures for broadband microwave circuit applications," *Microwave J.*, pp. 102–123, 1991.
- [17] *Sonnet em User's Manuals*, Sonnet Software, Liverpool, NY, 1997.
- [18] R. C. Neville, B. Hoeneisen, and C. A. Mead, "Permittivity of strontium titanate," *J. Appl. Phys.*, vol. 43, pp. 2124–2131, 1972.
- [19] A. B. Kozyrev, O. I. Soldatenkov, T. B. Samoilova, A. V. Ivanov, C. H. Mueller, T. V. Rivkin, and G. A. Koepf, "Response time and power handling capability of tunable microwave devices using ferroelectric thin-films," *Integrated Ferroelect.*, vol. 22, pp. 329–340, 1998.



Guru Subramanyam (S'82–M'94–SM'00) received the B.E. degree in electrical and electronics engineering from the University of Madras, Madras, India, in 1984, and the M.S. and Ph.D. degrees in electrical engineering from the University of Cincinnati, Cincinnati, OH, in 1988 and 1993, respectively. His doctoral dissertation concerned thallium-based high-temperature superconducting thin-films for microwave electronics applications.

In August 1993, he joined the University of Northern Iowa, Cedar Falls, where he remained until 1998. He is currently an Assistant Professor in the Department of Electrical and Computer Engineering, University of Dayton, Dayton, OH. His current research work is in the area of tunable components for K -band satellite communication systems. His areas of research include microelectronics, microwave electronics, and applied superconductivity.

Frederick W. Van Keuls (M'97) received the B.S. degree in physics and mathematics (*summa cum laude*) from Ohio State University, Columbus, in 1985, and the M.S. and a Ph.D. degrees in physics from Cornell University, Ithaca, NY, in 1987 and 1992, respectively. His doctoral dissertation concerned nuclear magnetic resonance (NMR) in ^3He films at low temperatures.

While at Cornell University, he was also an Instructor for electronics courses and a Post-Doctoral Researcher studying ^4He films in porous media. From 1993 to 1996, he investigated the electronic properties of two-dimensional GaAs/Al-GaAs heterostructures as a Research Associate at Case Western Reserve University. In 1996, he joined the Communications Technology Division, NASA Glenn Research Center, Cleveland, OH, as an NRC Research Associate, where, he has been designing, fabricating, and testing high-temperature superconducting and thin-film ferroelectric tunable microwave components, including frequency agile filters, tunable local oscillators, and phase shifters. He has co-authored over 40 publications.

Dr. Van Keuls is a member of the American Physical Society.



Félix A. Miranda (M'91–SM'98) received the B.S. degree in physics from the University of Puerto Rico, Rio Piedras, Puerto Rico, in 1983, the M.S. degree in physics from Rensselaer Polytechnic Institute, Troy, NY, in 1986, and the Ph.D. degree in physics from Case Western Reserve University, Cleveland, OH, in 1991.

In March 1991, he joined the NASA Lewis Research Center, as a member of the Solid-State Technology Branch. Since then, he has been involved with experimental research on the microwave and millimeter-wave properties of HTS thin films, HTS-based microwave components, and thin-film ferroelectric tunable microwave components. He is currently a Senior Research Scientist with the Electron Device Technology Branch, Communication Technology Division, NASA Glenn Research Center, Cleveland, OH. He spent the 1998–1999 academic year as a Visiting Professor of physics at the Humacao Campus, University of Puerto Rico. He has authored or co-authored over 60 technical publications in the areas of HTS thin films, dielectrics, and tunable ferroelectric microwave components, and has co-authored several book chapters. He is the co-inventor of three patent disclosures.

Dr. Miranda is a member of the American Physical Society, the Society of Hispanic Professional Engineers, and the Forum of Industrial and Applied Physicists. In 1998, he was the recipient of a NASA Administrator's Fellowship Program Award.